ACS Sustainable Chemistry & Engineering

Research Article

pubs.acs.org/journal/ascecg

Organic–Inorganic Hybrid Supramolecular Assembly: An Efficient Platform for Nonenzymatic Glucose Sensor

Meenakshi Choudhary, Sudheesh K. Shukla, Abu Taher, Samarjeet Siwal, and Kaushik Mallick*

Department of Chemistry, University of Johannesburg, P.O. Box 524, Auckland Park 2006, South Africa

Supporting Information

ABSTRACT: A polyaniline-supported copper(I) composite has been synthesized using a one-step chemical synthesis route under ambient conditions. The composite material was characterized using microscopic and spectroscopic techniques. The Cu(I)–polymer composite material was employed as a sensing material for a nonenzymatic glucose sensor. Compared with pure polyaniline, Cu(I)–polyaniline showed improved electrocatalytic activity toward glucose oxidation due to the integration of Cu(I) and that exhibited the enhanced anodic current.

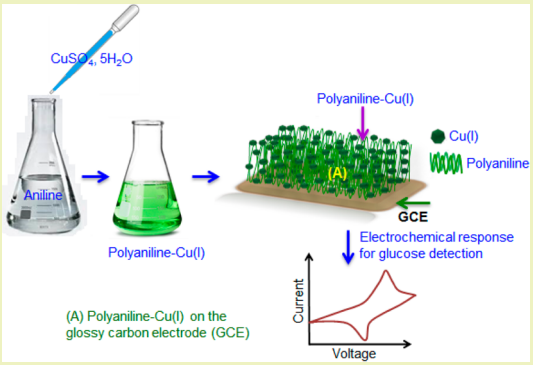

KEYWORDS: *Cu(I)–polymer, In situ synthesis, Glucose sensor, Nonenzymatic*

INTRODUCTION

Diabetes is a metabolic disorder resulting from insulin deficiency, reflected by blood glucose concentrations, and associated with long-term damage and failure of various organs especially the heart, kidney, eyes, and blood vessels.[1] The early as well as sensitive detection of abnormal glucose level in the blood is very important for proper treatment to reduce the above risks.

There are many approaches that have been developed to measure glucose concentration, such as optical,[2−4] capacitive detection,[5] electro-chemiluminescence,[6] colorimetric[7] and electrochemical techniques, but among them electrochemical sensing methods have received enormous attention due to their high sensitivity, simple instrumentation, low production cost, and rapid response speed.

The electrochemical method using glucose oxidase,[8−11] an enzymatic catalyst, has been widely used for glucose biosensor fabrication, and the activity of the enzyme can be easily affected by temperature, pH, humidity, and toxic chemicals.[12] There are also some disadvantages of the enzyme-modified electrodes (for enzymatic electrochemical experiment), such as instability, high cost of enzymes, complicated immobilization technique, and critical operating procedure. Therefore, considerable attention has been paid to develop the nonenzymatic electrochemical detection method to solve these problems that seems to be an extremely attractive alternative technique free from the above-mentioned drawbacks.

Recently, numerous nanostructured materials have been reported for developing nonenzymatic glucose sensors. The electrochemical detection of glucose using different noble metal nanoparticles as the electrocatalyst such as platinum[13,14] and gold[15,16] has been explored to develop enzyme-free sensors for glucose. Poly(vinyl alcohol)-stabilized silver nanoparticles also showed a viable alternative as a catalyst for electrochemical detection of glucose.[17] Various bimetallic systems such as Pt–Ir,[18] Pt–Pb,[19,20] and Pt–Ru[21] have also been involved as important strategic materials for the construction of non-enzymatic glucose sensors. Highly ordered nickel nanowire arrays were reported as the electrode material for electrochemical detection of glucose with good reproducibility and long-term stability.[22] Copper-based nanostructures, such as nanorods,[23] nanofibers,[24] and nanoclusters,[25] also offer excellent performance and have shown good catalytic activity for nonenzymatic oxidation of glucose. The unique properties of nanostructured materials are directly related to their size and are significantly different from their corresponding bulk materials.[26,27] Besides precise control of size, the stability of nanoparticles is an extremely important issue. To prevent the agglomeration of the nanomaterials, it is essential to have a robust support system for the particles to remain as individual. Carbon-based materials, such as carbon nanotubes, single-walled carbon nanotubes,[28] multiwalled carbon nanotubes,[29] and graphene,[30,31] provide excellent support for different nanostructured materials for glucose detection.

Besides the carbon-based solid support, polymers have also been employed to promote stabilization of the nanoparticles. There is growing interest in conducting polymers, which have shown numerous features for high performance biosensors.

Received: September 24, 2014
Revised: October 22, 2014
Published: October 31, 2014

Among the known conducting polymers, polyaniline and its derivatives have attracted intensive interest due to their excellent electronic properties, such as their π-conjugated backbone facilitating electron transfer and their doping adjustable electrical properties and metal-like transport properties at both room and low temperatures.[32] Polyaniline[33] and the polyaniline–hydrogel[34] system act as potential supports of metal nanoparticles for efficient detection of glucose. The incorporation of metal in the form of ionic particles or nanoparticles into polyaniline provides enhanced performance for both the host (polymer) and the guest (particle) that could lead to different physical properties and important potential applications. The paramagnetic property in highly protonic acid-doped polyaniline has been reported at low temperature,[35] whereas a similar magnetic behavior has also been reported by introducing metal nanoparticles[36,37] or metal ions[38] in the polyaniline matrix at room temperature. The Hall effect measurement of the gold–polyaniline sample confirms the conductivity characteristics of the polyaniline changed from "near insulator" to "low charge carrier density semiconductor" due to the addition of gold nanoparticles.[39]

Polyaniline also acts as an excellent platform for electrocatalysis reactions. A polyaniline film-modified electrode, doped with platinum group metals, was reported for the electrooxidation of methanol and other C-1 molecules.[40] The sandwich structure of Pd–polyaniline–Pd acts as an efficient electrocatalyst for the oxidation of ethanol.[41] The gold–polyaniline hybrid system performs as an electrocatalyst for the electrochemical oxidation of ascorbic acid and glucose oxidase.[42] Mercapto succinic acid-capped gold nanoparticle-doped polyaniline has been reported for excellent electrocatalytic efficiency with regard to the oxidation of β-nicotinamide adenine dinucleotide[43] and also for the detection of DNA hybridization using both electrochemical and surface plasmon-enhanced fluorescence spectroscopy methods.[44] The composite hollow structure of polyaniline and gold nanoparticles is an interesting material for the detection of dopamine, an important neurotransmitter in mammalian central nervous systems.[45]

In the present communication, we report an *in situ* synthesis technique for the preparation of Cu(I)–polyaniline supramolecular composite material by applying an "*in situ* polymerization and composite formation" (IPCF) type of reaction[46−50] using copper sulfate as an oxidizing agent for polymerizing aniline. During the polymerization process, each step is associated with a release of electrons and that reduces the Cu(II) ion to form Cu(I) ion. The Cu(I) ion, which acts as the catalytic center, binds with the chain nitrogen of the polyaniline and has been used as an electrocatalyst for the nonenzymatic detection of glucose.

EXPERIMENTAL SECTION

Materials. Aniline was distilled at a reduced pressure over zinc metal. The middle fraction was collected and stored at ∼10 °C under argon. Ultrapure water (specific resistivity >17 MΩcm) was used to prepare the solution of $CuSO_4$, $5H_2O$ (10^{-2} mol dm^{-3}). All the other chemicals were used as received.

Characterization Techniques. Scanning electron microscopy (SEM) studies were undertaken in a FEI FEG Nova 600 Nano lab at 5 kV. Transmission electron microscopy (TEM) studies of the particles were carried out at an accelerated voltage of 197 kV using a Philips CM200 TEM equipped with a LaB_6 source. An ultrathin windowed energy-dispersive X-ray spectrometer (EDS) and a Gatan imaging filter (GIF) attached to the TEM were used to determine the chemical composition of the samples. The UV–vis spectra were recorded using a Shimadzu UV-1800 UV–vis spectrophotometer with a quartz cuvette. Infrared (IR) spectra were collected utilizing a Shimadzu IRAffinity-1 with a resolution of 0.5 cm^{-1}. The X-ray diffraction (XRD) patterns were recorded on a Shimadzu XD-3A X-ray diffractometer operating at 20 kV using Cu Kα radiation (k = 0.1542 nm). The X-ray photoelectron spectra were collected in an ultrahigh vacuum chamber attached to a Physical Electronics PHI 560 ESCA/SAM system.

Electrochemical measurements were carried out with an Autolab PGSTAT 910 potentiostat connected to a data controller. A three-electrode system was used in the experiment with a "bare" and a "modified" glassy carbon electrode (GCE) as the working electrode. An Ag/AgCl electrode and a Pt wire electrode were used as the reference and counter electrodes, respectively. Prior to the electrode modification, the GCE was mechanically polished with α-Al_2O_3 powder in ethanol and water, respectively. The polished GCE was then electrochemically cleaned by cyclic voltammetry between −0.6 V to +0.6 V at 50 mV S^{1-} in a 0.05 M phosphate buffered saline (PBS) solution until stable cyclic voltammogram were obtained.

Preparation of Cu(I)–Polyaniline Composite Catalyst. In a typical experiment, a required amount of aniline (10^{-2} mol dm^{-3}) was diluted in 25 mL methanol in a conical flask. To this, a $CuSO_4$, $5H_2O$ solution in water (10^{-2} mol dm^{-3}) was added by maintaining a molar concentration ratio 1:1 (aniline and copper sulfate) slowly under continuous stirring conditions. During the addition, the solution took on a green colorization, while at the end, a parrot green precipitation was formed at the bottom of the conical flask. The entire reaction was performed at room temperature and under open atmosphere. The material was allowed to settle for 10 min after which 5 μL of the colloidal solution was taken from the bottom of the conical flask and pipetted onto lacey, carbon-coated, Ni-mesh grids for TEM characterization. Subsequent to the TEM study, the same grids were sputter coated with a conducting layer of Au–Pd a few nanometers thick and was viewed by scanning electron microscopy (SEM). The required amount of material was used for UV–vis and IR spectroscopy studies. A total of 2 mL of the above colloidal solution was transferred from the conical flask to a small sample vial for the electrochemical glucose detection experiment. The remaining portion of the compound was dried under vacuum at 60 °C and used for XRD and XPS characterization.

Fabrication of Modified Electrode. The working electrode was modified by the "drop and dry" method using the Cu(I)–Polyaniline composite as an electrocatalyst and then allowed to dry at room temperature. After every run, the electrode was washed, and an equal amount (5 μL) of new catalyst was applied on the electrode for the next study.

RESULTS AND DISCUSSION

Optical and Microscopic Properties of the Cu(I)–Polyaniline Composite Material. We have examined the spectroscopic behavior of the dried material by IR analysis within the spectral range from 2000 to 500 cm^{-1} (Figure 1A). IR analysis is useful for examining the resonance modes of the benzenoid and quinoid units and the bonds, such as out-of-plane C–H and C–N of the polyaniline compound. In the IR spectra of the resultant compound, the peak at 1635 cm^{-1} corresponds to the group N=Q=N (where Q represents a quinoid ring), while the N–B–N group (where B represents a benzenoid ring) absorbs at 1500 cm^{-1}. A small peak, with an equivalent intensity of the N–B–N group, observed at 1398 $cm^{-1}$is due to the presence of the C–N^+ polaron conducting species in the polyaniline structure.[51] The peaks at 1110 and 1018 cm^{-1} correspond to the aromatic C–H in-plane bending vibration of permigraniline state of polyaniline, whereas the vibrational band at 1265 cm^{-1} is related to the protonated C–N group.[52,53] The bands at 765 and 708 cm^{-1} are due to an

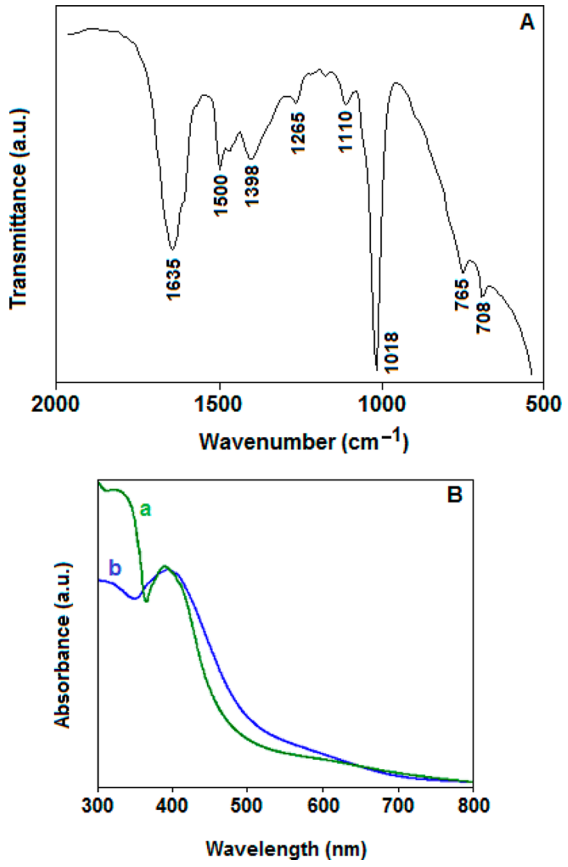

Figure 1. (A) FTIR spectrum of Cu(I)−polyaniline compound within the spectral range from 2000 to 500 cm^{-1}. In the IR spectra, the peak at 1635 cm^{-1} corresponds to the quinoid ring, while the N−B−N group represents the benzenoid ring at 1500 cm^{-1}. (B) In the UV−vis spectra, for both of the samples, (a) Cu(I)−polyaniline and (b) pure polyaniline, a shoulder-like feature has been appeared in the range of 300−330 nm that corresponds to $\pi-\pi^*$ transition of benzenoid rings. A prominent broad peak at about 400 nm observed in the samples represent polaron−bipolaron transition of the polymer.

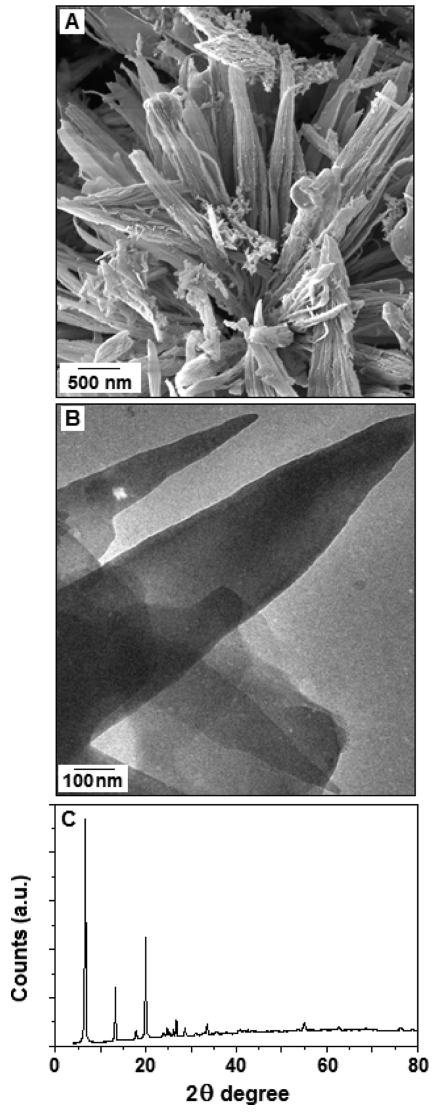

Figure 2. (A) SEM image of the Cu(I)−polyaniline composite material, which illustrates like the *Aloe vera* leaf-like morphology. (B) TEM image of the Cu(I)−polyaniline composite material with a smooth morphology and no evidence of formation of copper nanoparticles. (C) XRD pattern confirms the crystalline character of the polyaniline, and there is no indication for the formation of metallic copper.

aromatic out-of-plane C−H deformation vibration and are related to the substituted benzene ring. These results are in good agreement with previously reported IR-spectroscopic characterization data of polyaniline.[51−53] In the UV−vis spectra (Figure 1B), for both of the samples, Cu(I)−polyaniline and pure polyaniline, a shoulder-like feature has appeared in the range of 300−330 nm that corresponds to the $\pi-\pi^*$ transition of benzenoid rings. A prominent broad peak at about 400 nm has also been observed in both the samples that represent the polaron−bipolaron transition of the polymer. A weak absorption band has been observed within the range between 500−750 nm, which indicates the benzenoid to quinoid excitonic transition in both samples.[54] The UV−vis spectrum also corroborates with the previously reported spectrum data of polyaniline.[55]

The SEM image (Figure 2A) of the resultant polyaniline-based material illustrates the *Aloe vera* leaf-like morphology. From the TEM image in Figure 2B, no evidence has been found for the presence of copper nanoparticles in the resultant material. The sample was also characterized with X-ray diffraction (XRD) analysis (Figure 2C). The XRD pattern confirms the crystalline character of the polyaniline, and there is no indication for the formation of the metallic copper. The EDS spectra (Figure 3A) derived from placing the electron beam in the different areas of the material and the presence of a copper peak with almost equal intensity indicates the homogeneous distribution of copper within the sample. The Ni peaks are derived from the TEM support grid. The XPS spectrum shows the asymmetric nature of the Cu $2p_{3/2}$ peak that suggests the presence of more than one valence state of copper is present in the sample (Figure 3B, inset). The main peak at 932.45 eV corresponds to Cu(I), and a shoulder-like appearance at 933.65 eV represents the presence of a minute amount of unreacted Cu(II).[56,57] Area calculations indicate that 92% of the Cu(I) ions were present in the sample, with the remaining 8% being unreacted Cu(II) ions. Considering the results from the optical and microscopic characterization, we have conclude the formation of the Cu(I)−polyaniline composite material.

Cu(I)−Polyaniline as an Electrocatalyst for Non-enzymatic Glucose Detection. In the present work, we

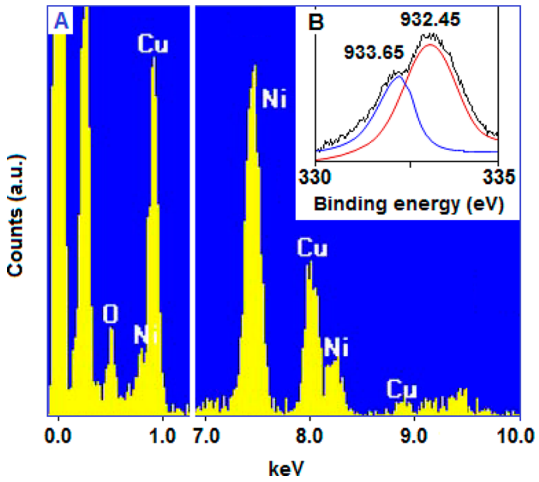

Figure 3. (A) EDX spectrum obtained from the electron beam being focused onto various locations of the polymer surface indicates the presence of copper all over the polymer in similar concentrations. (B) X-ray photoelectron spectroscopy (XPS) analysis shows the asymmetric nature of the Cu $2p_{3/2}$ peak that suggests the presence of more than one valence state of copper is present in the sample (inset). The main peak at 932.45 eV corresponds to Cu(I), and a shoulder-like appearance at 933.65 eV represents the presence of Cu(II). Area calculation indicates that 92% of the Cu(I) ions were present in the sample, with remaining 8% being unreacted Cu(II) ions.

have compared the affinity and sensitivity of polyaniline, synthesized using ammonium persulfate, and Cu(I)−polyaniline for the electrochemical detection of glucose. For this, the first cyclic voltammetry (CV) technique has been employed to test the barrier kinetics of the catalytic interface using the electroactive species $[Fe(CN)_6]^{3-/4-}$ (FCN). The extent of kinetic hindrance to the electron transfer process increases with increasing film thickness and decreases with the defect density of the barrier. The CV responses of 0.5 mM of FCN at bare GCE, polyaniline-modified GCE, and Cu(I)−polyaniline-modified GCE at pH 7.5, operating at a scan rate of 50 mVs^{-1}, are shown in Figure S1 (A) of the Supporting Information. After modifying the electrode with polyaniline, a decrease in the redox peak current was observed (curve b), indicating that the polyaniline acts as an electron and mass transfer blocking layer and thus hinders the diffusion of ferricyanide toward the electrode surface. In contrast, for the Cu(I)−polyaniline-modified electrode, the voltammetric response of ferricyanide (curve c) is restored close to that obtained at the bare GCE (curve a). This demonstrates that Cu(I) has been successfully assembled on the electrode surface and provides the necessary conduction pathway to promote the electron transfer between the analyte (ferricyanide) and the electrode surface. The decreasing peak height indicates the passivation of the electrode surface. The cyclic voltammogram of the Cu(I)−polymer-modified GC electrode in the presence of FCN (5 mM) containing the PBS (50 mM) electrolyte with the scan rates varying from 10 to 250 mVs^{-1} are shown in Figure S1 (B) of the Supporting Information. From the figure, it is clear that the current intensity (peak height) is directly proportional with the scan rate, which suggest that the kinetics of the ferrocyanide (FC) is diffusion controlled on the Cu(I)−polyaniline-modified GCE. The peak-to-peak (anodic and cathodic) separation becomes wider with increasing scan rates, and the peak currents for both the anode and the cathode increasingly shift toward high current values. The results indicate that the surface adsorption of the FCN ion dominates the electrochemical kinetics where the charge transfer was under diffusion controlled.

The electrocatalytic activity of bare, polyaniline, and Cu(I)−polyaniline-modified GC electrodes were recorded separately in the absence (Figure 4A, inset) and the presence (Figure 4B) of

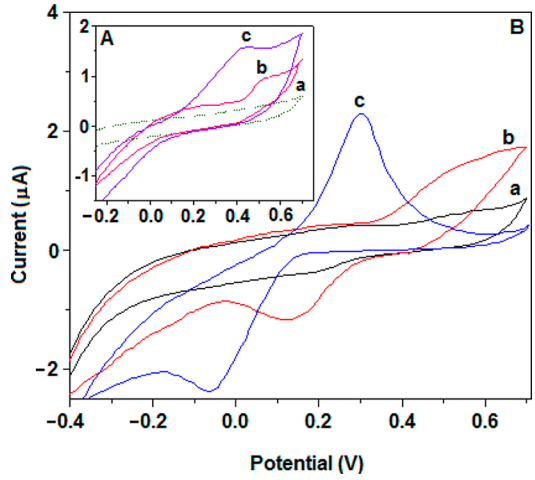

Figure 4. Cyclic voltammograms of (a) bare GCE, (b) polyaniline-modified GCE, and (c) Cu(I)−polyaniline-modified GCE in the absence (A), inset, and (B) in the presence of glucose (1.0 mM) in milli-Q water under the scan rate of 50 mV^{-1}.

glucose at a scan rate of 50 mVs^{-1} in milli-Q water. In Figure 4A, curve (a), for the bare electrode, no anodic peak current has been noticed. In curve (b), for the polyaniline-modified GC electrode, a slight enhancement of the anodic current value has been observed, indicating the electro-oxidation of the polyaniline. For the Cu(I)−polyaniline-modified GC electrode, a further increment of the anodic peak current indicates the effect of oxidation for both the polyaniline and monovalent copper species. In Figure 4B, with the presence of 1.0 mM glucose, no improvement of the anodic current has been found, as compared with the previous experiment, for the bare GC electrode, curve (a). The polyaniline-modified electrode shows a slight enhancement of the peak current [0.45 μA, measured at 0.650 V, Figure 4B, curve (b)] in the presence of glucose when compared with the similar electrode in absence of glucose. The Cu(I)−polyaniline-modified GC electrode exhibited enhanced electrocatalytic oxidation of glucose with the anodic peak current value 2.35 μA at the applied potential value 0.300 V [Figure 4B, curve (c)]. These results indicated that Cu(I)−polyaniline exhibited excellent electrocatalytic activity toward the oxidation of glucose, and such enhanced activity is due to the introduction of copper ion, which promotes the electron transfer process.

Figure 5A represents the CV responses obtained from the different concentrations of glucose at the Cu(I)−polyaniline-modified electrode at a scan rate of 50 mVs^{-1} in milli-Q water. With increasing the amount of glucose concentration, 1, 2, 4, 6, 8, and 10 mM, to the electrolyte, the periodic enhancement of the anodic peak current with a regression coefficient (R^2) of 0.9902 suggests that the electrocatalytic activity of Cu(I)−polyaniline is dependent on the analyte concentration (Figure 5A). The increase in anodic current is attributed to the electro-oxidation of glucose to glucolactone, which is accompanied by the oxidation of Cu(I) to Cu(II). As the electro-oxidation of

dx.doi.org/10.1021/sc500613q | ACS Sustainable Chem. Eng. 2014, 2, 2852−2858

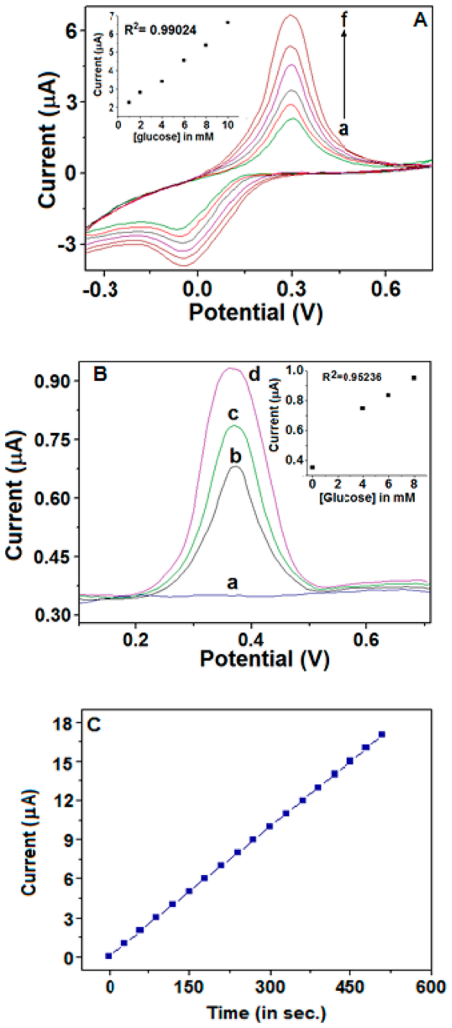

Figure 5. (A) Cyclic voltammograms of Cu(I)−polyaniline-modified GCE in the presence of glucose with the concentration of (a) 1, (b) 2, (c) 4, (d) 6, (e) 8, and (f) 10 mM in milli-Q water under the scan rate of 50 mVs^{-1}. (B) Square wave voltammograms of glucose of various concentrations (a) 0, (2) 4.0, (3) 6.0, and (4) 8.0 mM in milli-Q water under the frequency of 10 Hz using Cu(I)−polyaniline-modified GC working electrodes. (C) Current response, with the successive addition of glucose, as a function of time at a constant voltage of (+) 0.200 V in the presence of a Cu(I)−polyaniline-modified working electrode.

glucose consumes Cu(II), a slight decrease in the cathodic peak current occurs. The electrocatalytic properties of Cu(I)−polyaniline was also studied by a square wave voltammetry (SWV) technique using various amounts of glucose concentration at the frequency of 10 Hz. Our result indicates that the SWV technique is not as sensitive as the CV technique for the detection of low concentration of glucose using the composite material as a catalyst. At higher glucose concentration, clear and distinct current peaks (with R^2 = 0.95236) can be seen at around ∼0.365 V for the analyte concentrations of 4 mM (curve b), 6 mM (curve c), and 8 mM (curve d) (Figure 5B). In the absence of glucose, no characteristic peak has been observed in the potential zone (Figure 5B, curve a). Figure 5C illustrates the current response, with the successive addition of glucose, as a function of time at a constant voltage of (+) 0.200 V in the presence of the Cu(I)−polyaniline-modified working electrode. A steady increase in current response has been observed with the addition of glucose to the electrolyte (milli-Q water) from 0.4 to 4.0 mM, which is much lower than the normal physiological level of glucose (4.4 to 6.6 mM),[58] with a sensitivity value of 0.4744 μA mM^{-1} cm^{-2}. The comparative performance of different electrocatalysts used for the nonenzymatic detection of the glucose is summarized in Table 1 of the Supporting Information. The above results indicate that the Cu(I)−polyaniline composite could be a potential material for the fabrication of a nonenzymatic glucose sensor device in terms of performance and sensitivity. We have also performed the "effect of pH" study of the catalyst and found that the Cu(I)−polyaniline composite is tolerant under acidic and basic conditions within a pH range from 2 to 12 for the detection of glucose.

CONCLUSIONS

In summary, an efficient route for the synthesis of a polyaniline-supported copper(I) composite material has been described under ambient conditions. The supramolecular material was successfully applied as an electrocatalyst, with high sensitivity, fast response, low detection limit, and good stability, for the nonenzymatic electrochemical detection of glucose. The simple preparation procedure and use of a low-cost precursor of the composite could mean the material is a promising candidate for the fabrication of an economical glucose-sensing device. We envision that the above-mentioned organic−inorganic hybrid system could be highly useful for a wide range of applications in bioelectronics and future generation energy storage electrodes for nonenzymatic glucose fuel cells.

ASSOCIATED CONTENT

Supporting Information

Additional figure and table. This material is available free of charge via the Internet at http://pubs.acs.org.

AUTHOR INFORMATION

Corresponding Author

* E-mail: kaushikm@uj.ac.za. Tel: +27 11 5592368. Fax: +27 11 5592819.

Notes

The authors declare no competing financial interest.

ACKNOWLEDGMENTS

The authors (M.C., S.K.S., A.T., S.S., and K.M.) acknowledge financial support from the Research Committee and the Faculty of Science of the University of Johannesburg. M.C. also acknowledges financial support from the National Research Foundation, South Africa. A.T. and S.S. further acknowledge financial support from the Global Excellence and Stature fellowship from the University of Johannesburg.

REFERENCES

(1) Chen, C.; Xie, Q.; Yang, D.; Xiao, H.; Fu, Y.; Tan, Y.; Yao, S. Recent advances in electrochemical glucose biosensors: A review. *RSC Adv.* **2013**, *3*, 4473−4491.

(2) Song, C.; Pehrsson, P. E.; Zhao, W. Optical enzymatic detection of glucose based on hydrogen peroxide-sensitive HiPco carbon nanotubes. *J. Mater. Res.* **2006**, *21*, 2817−2823.

(3) Barone, P. W.; Parker, R. S.; Strano, M. S. In vivo fluorescence detection of glucose using a single-walled carbon nanotube optical sensor: Design, fluorophore properties, advantages, and disadvantages. *Anal. Chem.* **2005**, *77*, 7556−7562.

(4) Shen, X. W.; Huang, C. Z.; Li, Y. F. Localized surface plasmon resonance sensing detection of glucose in the serum samples of

diabetes sufferers based on the redox reaction of chlorauric acid. *Talanta* **2007**, *72*, 1432−1437.
(5) Cheng, Z.; Wang, E.; Yang, X. Capacitive detection of glucose using molecularly imprinted polymers. *Biosens. Bioelectron.* **2001**, *16*, 179−185.
(6) Kremeskotter, J.; Wilson, R.; Schiffrin, D. J.; Luff, B. J.; Wilkinson, J. S. Detection of glucose via electrochemiluminescence in a thin-layer cell with a planer optical waveguide. *Meas. Sci. Technol.* **1995**, *6*, 1325−1328.
(7) Morikawa, M.; Kimizuka, N.; Yoshihara, M.; Endo, T. New colorimetric detection of glucose by means of electron-accepting indicators: Ligand substitution of $[Fe(acac)_{3-n}(phen)_n]^{n+}$ complexes triggered by electron transfer from glucose oxidase. *Chem: Eur. J.* **2002**, *8*, 5580−5584.
(8) Kaushik, A.; Khan, R.; Solanki, P.; Pandey, P.; Alam, J.; Ahmad, S.; Malhotra, B. D. Iron oxide nanoparticles-chitosan composite based glucose biosensor. *Biosens. Bioelectron.* **2008**, *24*, 676−683.
(9) Hocevar, S. B.; Ogorevc, B.; Schachl, K.; Kalcher, K. Glucose microbiosensor based on MnO_2 and glucose oxidase modified carbon fiber microelectrode. *Electroanalysis* **2004**, *16*, 1711−1716.
(10) Umar, A.; Rahman, M. M.; Al-Hajry, A.; Hahn, Y. B. Enzymatic glucose biosensor based on flower-shaped copper oxide nanostructures composed of thin nanosheets. *Electrochem. Commun.* **2009**, *11*, 278−281.
(11) Zhang, X. J.; Wang, G. F.; Zhang, W.; Hu, N. J.; Wu, H. Q.; Fang, B. Seed-mediated growth method for epitaxial array of CuO nanowires on surface of Cu nanostructures and its application as a glucose sensor. *J. Phys. Chem., C* **2008**, *112*, 8856−8862.
(12) Wilson, R.; Turner, A. P. F. Glucose oxidase: An ideal enzyme. *Biosens. Bioelectron.* **1992**, *7*, 165−185.
(13) Park, S.; Chung, T. D.; Kim, H. C. Nonenzymatic glucose detection using mesoporous platinum. *Anal. Chem.* **2003**, *75*, 3046−3049.
(14) Yuan, J. H.; Wang, K.; Xia, X. H. Highly ordered platinum-nanotubule arrays for amperometric glucose sensing. *Adv. Funct. Mater.* **2005**, *15*, 803−809.
(15) Bai, Y.; Yang, W.; Sun, Y.; Sun, C. Enzyme-free glucose sensor based on a three-dimensional gold film electrode. *Sens. Actuators, B* **2008**, *134*, 471−476.
(16) Yin, H.; Zhou, C.; Xu, C.; Liu, P.; Xu, X.; Ding, Y. Aerobic oxidation of d-glucose on support-free nanoporous gold. *J. Phys. Chem., C* **2008**, *112*, 9673−9678.
(17) Guascito, M. R.; Chirizzi, D.; Picca, R. A.; Mazzotta, E.; Malitesta, C. Ag nanoparticles capped by a nontoxic polymer: Electrochemical and spectroscopic characterization of a novel nanomaterial for glucose detection. *Mater. Sci. Eng., C* **2011**, *31*, 606−611.
(18) Holt-Hindle, P.; Nigro, S.; Asmussen, M.; Chen, A. Amperometric glucose sensor based on platinum−iridium nanomaterials. *Electrochem. Commun.* **2008**, *10*, 1438−1441.
(19) Cui, H. F.; Ye, J. S.; Zhang, W. D.; Li, C. M.; Luong, J. H. T.; Sheu, F. S. Selective and sensitive electrochemical detection of glucose in neutral solution using platinum−lead alloy nanoparticle/carbon nanotube nanocomposites. *Anal. Chim. Acta* **2007**, *594*, 175−183.
(20) Bai, Y.; Sun, Y.; Sun, C. Pt−Pb nanowire array electrode for enzyme-free glucose detection. *Biosens. Bioelectron.* **2008**, *24*, 579−585.
(21) Li, L.-H.; Zhang, W.-D.; Ye, J.-S. Electrocatalytic oxidation of glucose at carbon nanotubes supported PtRu nanoparticles and its detection. *Electroanalysis* **2008**, *20*, 2212−2216.
(22) Lu, L.-M.; Zhang, L.; Qu, F.-L.; Lu, H.-X.; Zhang, X.-B.; Wu, Z.-S.; Huan, S.-Y.; Wang, Q.-A.; Shen, G.-L.; Yu, R.-Q. A nano-Ni based ultrasensitive nonenzymatic electrochemical sensor for glucose: Enhancing sensitivity through a nanowire array strategy. *Biosens. Bioelectron.* **2009**, *25*, 218−223.
(23) McAuley, C.; Du, Y.; Wildgoose, G. G.; Compton, R. G. The use of copper(II) oxide nanorod bundles for the non-enzymatic voltammetric sensing of carbohydrates and hydrogen peroxide. *Sens. Actuators, B* **2008**, *135*, 230−235.
(24) Wang, W.; Zhang, L.; Tong, S.; Li, X.; Song, W. Three-dimensional network films of electrospun copper oxide nanofibers for glucose determination. *Biosens. Bioelectron.* **2009**, *25*, 708−714.
(25) Kang, X.; Mai, Z.; Zou, X.; Cai, P.; Mo, J. A sensitive nonenzymatic glucose sensor in alkaline media with a copper nanocluster/multiwall carbon nanotube-modified glassy carbon electrode. *Anal. Biochem.* **2007**, *363*, 143−150.
(26) Service, R. F. Materials science: Small clusters hit the big time. *Science* **1996**, *271*, 920−922.
(27) Schmid, G.; Corain, B. Nanoparticulated gold: Syntheses, structures, electronics, and reactivities. *Eur. J. Inorg. Chem.* **2003**, *17*, 3081−3098.
(28) Zeng, Z.; Zhou, X.; Huang, X.; Wang, Z.; Yang, Y.; Zhang, Q.; Boey, F.; Zhang, H. Electrochemical deposition of Pt nanoparticles on carbon nanotube patterns for glucose detection. *Analyst* **2010**, *135*, 1726−1730.
(29) Zhang, X.; Wang, G.; Huang, Y.; Yu, L.; Fang, B. Non-enzymatic glucose detection using Ni/multi-walled carbon nanotubes composite. *Micro Nano Lett.* **2012**, *7*, 168−170.
(30) Zhang, H.; Xu, X.; Yin, Y.; Wu, P.; Cai, C. Nonenzymatic electrochemical detection of glucose based on Pd_1Pt_3−graphene nanomaterials. *J. Electroanal. Chem.* **2013**, *690*, 19−24.
(31) Lu, X.; Ye, Y.; Xie, Y.; Song, Y.; Chen, S.; Li, P.; Chen, L.; Wang, L. Copper coralloid granule/polyaniline/reduced graphene oxide nanocomposites for nonenzymatic glucose detection. *Anal. Methods.* **2014**, *6*, 4643−4651.
(32) Lee, K.; Cho, S.; Park, S. H.; Heeger, A. J.; Lee, C. W.; Lee, S. H. Metallic transport in polyaniline. *Nature* **2006**, *441*, 65−68.
(33) Xian, Y.; Hu, Y.; Liu, F.; Xian, Y.; Wang, H.; Jin, L. Glucose biosensor based on Au nanoparticles−conductive polyaniline nanocomposite. *Biosens. Bioelectron.* **2006**, *21*, 1996−2000.
(34) Zhai, D.; Liu, B.; Shi, Y.; Pan, L.; Wang, Y.; Li, W.; Zhang, R.; Yu, G. Highly sensitive glucose sensor based on Pt nanoparticle/polyaniline hydrogel heterostructures. *ACS Nano* **2013**, *7*, 3540−3546.
(35) Sariciftci, N. S.; Heeger, A. J.; Cao, Y. Paramagnetic susceptibility of highly conducting polyaniline: Disordered metal with weak electron-electron interactions (Fermi glass). *Phys. Rev., B* **1994**, *49*, 5988.
(36) Mallick, K.; Witcomb, M.; Strydom, A. In situ formation of magnetic−luminescent, bi-functional, polymer-stabilized cerium sulfide nanoparticles. *Appl. Phys. A: Mater. Sci. Process.* **2012**, *109*, 607−611.
(37) Mallick, K.; Witcomb, M.; Erasmus, R.; Strydom, A. Low temperature magnetic property of polymer encapsulated gold nanoparticles. *J. Appl. Phys.* **2009**, *106*, 074303.
(38) Mallick, K.; Witcomb, M.; Scurrell, M.; Strydom, A. Paramagnetic polyaniline nanospheres. *Chem. Phys. Lett.* **2010**, *494*, 232−236.
(39) Mallick, K.; Witcomb, M.; Scurrell, M.; Strydom, A. Optical, microscopic and low temperature electrical property of one-dimensional gold−polyaniline composite networks. *J. Phys. D: Appl. Phys.* **2009**, *42*, 095409.
(40) Laborde, H.; Leger, J. M.; Lamy, C. Electrocatalytic oxidation of methanol and C1 molecules on highly dispersed electrodes Part II: Platinum-ruthenium in polyaniline. *J. Appl. Electrochem.* **1994**, *24*, 1019−1027.
(41) Wang, A.-L.; Xu, H.; Feng, J.-X.; Ding, L.-X.; Tong, Y.-X.; Li, G.-R. Design of Pd/PANI/Pd sandwich-structured nanotube array catalysts with special shape effects and synergistic effects for ethanol electrooxidation. *J. Am. Chem. Soc.* **2013**, *135*, 10703−10709.
(42) Granot, E.; Katz, E.; Basnar, B.; Willner, I. Enhanced bioelectrocatalysis using au-nanoparticle/polyaniline hybrid systems in thin films and microstructured rods assembled on electrodes. *Chem. Mater.* **2005**, *17*, 4600−4609.
(43) Tian, S.; Liu, J.; Zhu, T.; Knoll, W. Polyaniline doped with modified gold nanoparticles and its electrochemical properties in neutral aqueous solution. *Chem. Commun.* **2003**, 2738−2739.

(44) Tian, S.; Liu, J.; Zhu, T.; Knoll, W. Polyaniline/gold nanoparticle multilayer films: Assembly, properties, and biological applications. *Chem. Mater.* **2004**, *16*, 4103−4108.
(45) Feng, X.; Mao, C.; Yang, G.; Hou, W.; Zhu, J.-J. Polyaniline/Au composite hollow spheres: Synthesis, characterization, and application to the detection of dopamine. *Langmuir* **2006**, *22*, 4384−4389.
(46) Mallick, K.; Witcomb, M.; Scurrell, M. Fabrication of a nanostructured gold-polymer composite material. *Eur. Phys. J. E: Soft Matter Biol. Phys.* **2006**, *20*, 347−353.
(47) Mallick, K.; Witcomb, M.; Scurrell, M.; Strydom, A. M. In-situ chemical synthesis route for a fiber shaped gold-polyaniline nanocomposite. *Gold Bull.* **2008**, *41*, 246−250.
(48) Mallick, K.; Witcomb, M. J.; Scurrell, M. S. Directional assembly of polyaniline functionalized gold nanoparticles. *J. Phys: Condens. Matter.* **2007**, *19*, 196225.
(49) Mallick, K.; Witcomb, M. J.; Erasmus, R.; Scurrell, M. S. Hydrophilic behaviour of gold-poly (o-phenylenediamine) hybrid nanocomposite. *Mater. Sci. Eng., B* **2007**, *140*, 166−171.
(50) Mallick, K.; Witcomb, M. J.; Strydom, A. M. Charge transport property of one-dimensional gold−polyaniline composite networks. *Phys. Status. Solidi., A* **2009**, *206*, 2245−2248.
(51) Oliveira, M. M.; Castro, E. G.; Canestraro, C. D.; Zanchet, D.; Ugarte, D.; Roman, L. S.; Zarbin, A. A simple two-phase route to silver nanoparticles/polyaniline structures. *J. Phys. Chem., B* **2006**, *110*, 17063−17069.
(52) Mallick, K.; Witcomb, M. J.; Scurrell, M. S. Formation of palladium nanoparticles in poly (o-methoxyaniline) macromolecule fibers: An in-situ chemical synthesis method. *Eur. Phys. J. E: Soft Matter Biol. Phys.* **2006**, *19*, 149−154.
(53) Lei, Z.; Zhang, H.; Ma, S.; Ke, Y.; Li, J.; Li, F. Electrochemical polymerization of aniline inside ordered macroporous carbon. *Chem. Commun.* **2002**, 676−677.
(54) Huang, J.; Moore, J. A.; Acquaye, J. H.; Kaner, R. B. Mechanochemical route to the conducting polymer polyaniline. *Macromolecules* **2005**, *38*, 317−321.
(55) Pillalamarri, S. K.; Blum, F. D.; Tokuhiro, A. T.; Bertino, M. F. One-pot synthesis of polyaniline−metal nanocomposites. *Chem. Mater.* **2005**, *17*, 5941−5944.
(56) Goodby, B.; Pemberton, J. XPS characterization of a commercial $Cu/ZnO/Al_2O_3$ catalyst: effects of oxidation, reduction, and the steam reformation of methanol. *Appl. Spectrosc.* **1988**, *42*, 754−760.
(57) Ong, W. L.; Huang, H.; Xiao, J.; Zeng, K.; Ho, G. W. Tuning of multifunctional Cu-doped ZnO films and nanowires for enhanced piezo/ferroelectric-like and gas/photoresponse properties. *Nanoscale* **2014**, *6*, 1680−1690.
(58) Li, J.; Liu, C. Y. Ag/Graphene heterostructures: Synthesis, characterization and optical properties. *Eur. J. Inorg. Chem.* **2010**, *8*, 1244−1248.